Vol.65: e22220061, 2022
https://doi.org/10.1590/1678-4324-2022220061
ISSN 1678-4324 Online Edition

Article - Engineering, Technology and Techniques

Linear AC Three-Phase OPF Model for Active Distribution Networks with Unbalanced ZIP Loads

Rafael Silva Pinto[1]*
https://orcid.org/0000-0002-0574-1444

Clodomiro Unsihuay-Vila [1]
https://orcid.org/0000-0002-1639-7765

Thelma Solange Piazza Fernandes[1]
https://orcid.org/0000-0002-5167-1547

Antonio Rubens Baran Junior [1]
https://orcid.org/0000-0001-8085-0678

[1]Universidade Federal do Paraná (UFPR), Departamento de Engenharia Elétrica, Curitiba, Paraná, Brasil.

Editor-in-Chief: Alexandre Rasi Aoki
Associate Editor: Alexandre Rasi Aoki

Received: 16-Mar-2022; Accepted: 23-May-2022.

*Correspondence: rafael.pinto@ufpr.br (R.S.P.).

HIGHLIGHTS

- An AC linear optimal power flow model for unbalanced ZIP loads.
- Model includes voltage regulators, distributed generation, and mutual impedance.
- Results show deviations lower than 0.6% for voltage magnitude compared to a non-linear model.
- Results show deviations lower than 3% for voltage angle compared to a non-linear model.

Abstract: Although nonlinear Alternating Current (AC) Optimal Power Flow (OPF) may provide more accurate results compared to linearized OPF models, many ACOPF problems are complex and may require high, sometimes infeasible, computational time. The linear Direct Current OPF (DCOPF) has been widely used in power system analysis; however, it has limitations regarding reactive power analysis, and it may cause significant error in distribution networks with a high R/X ratio of feeders. Moreover, most of the existing formulations for the linear ACOPF do not consider mutual impedance for the lines and simplify the network as a single-phase system, which does not significantly represent unbalanced loads. This paper proposes a novel linear AC three-phase OPF formulation for unbalanced ZIP loads using current injection and considering delta and wye loads. The formulation is extended to include shunt capacitors, voltage regulators, and mutual impedance. The proposed methodology is illustrated using the IEEE 123-bus test system in case studies including/not-including voltage regulators, distributed generation, high R/X ratio, and mutual impedance. The results are very accurate compared with a nonlinear three-phase ACOPF model. The high computational performance and the accuracy of the proposed model considering distributed generation and high R/X ratio show its effectiveness in active distribution networks.

Keywords: Three-phase Power Flow; Unbalanced Load; Linear Optimal Power Flow; Power Flow Current Formulation.

INTRODUCTION

Optimal power flow (OPF) is an indispensable tool in power system operation and planning. The nonlinear alternating current (AC) OPF model is a complex, nonlinear, and nonconvex optimization problem, and it may require high computational effort. One of the most used linear models is the direct current (DC) OPF, which has been formulated in the analysis, operation, and expansion planning of electric power systems. The development of smart grids and active distribution networks (ADNs) leads to the attention of advanced OPF tools for monitoring, planning, and controlling the network. The ADNs have larger resistance to reactance (R/X) ratio as compared to the transmission networks; thus, the DCOPF is less accurate than the ACOPF for these networks [1,2]. Moreover, the DCOPF does not provide information regarding the reactive power flow and the voltage profile, and this information may play an important role in electric power systems when it comes to modern ADN.

Although DCOPF has limitations, mainly in distribution systems, linear models are commonly desired, because they require lower computational effort compared with nonlinear models. Besides, most recent works have been using linear ACOPF models in complex formulations for microgrids and ADN [3,4].

The ADN takes advantage of modern technology and communication to manage proactively the access to the distributed energy resources. It can coordinate intermittent distributed renewable generation units, distributed energy storage devices, and include other technologies to achieve the most suitable and economical operation [5]. Moreover, ADN generally has unbalanced ZIP loads. Therefore, in this context, modern distribution networks became a three-phase complex system, in which the linear AC three-phase OPF (L-3φ-ACOPF) formulation may be preferred, since it provides reactive power flow and voltage magnitude information with high computational performance.

In the three-phase power system, a more general type of load is often described as ZIP load, which is represented as a load with three distinct parts: a constant impedance portion (Z), a constant current portion (I), and a constant power portion (P). Each of these portions responds differently to changes in the load voltage. Therefore, single-phase representation does not significantly represent all types of loads, such as unbalanced loads.

In order to calculate the linear AC power flow, many works have formulated the balance equations using power injection in the nodes [6–9], some works have formulated them using current injection [10–14], few works proposed solving them using symmetrical components [15] for the three-phase representation, and some works have modeled them using the power injection with a decomposition technique [16,17] or heuristics [18].

Table 1 presents a summary of works related to the linear AC power flow. Each work is described if its formulation is based on power (P) or current (I) injection, if it uses single-phase (S) or three-phase (T) representation of the system, if it is applied symmetrical components (SC) for the three-phase case, if it is proposed a formulation for the load flow (LF) or the optimal power flow (OPF), if it is considered mutual impedance between the lines (MI) for the three-phase formulation, if the problem is formulated as linear or not (LP), if it is considered capacitors (CP), and voltage regulators (VR).

Most of the works in Table 1 formulate the load flow (LF) instead of the OPF [6–12,14,17]. In the load flow calculation is obtained the voltage magnitudes and angles using specified\known load and generator conditions. In the OPF there is an objective function, and the operational condition is found for the optimal value of this objective function. Therefore, OPF calculation is more likely to be used in the operational or expansion planning of the system.

Furthermore, the works that formulate linear power flow equations based on current injection do not consider mutual impedance. And these works do not explicitly include capacitors and voltage regulators in their formulation simultaneously, as well as they do not present the obtained results from this case study.

In this context, this paper proposes a new formulation for the L-3φ-ACOPF with unbalanced ZIP loads using current injection and considering delta and wye loads. The proposed model is also extended to incorporate shunt capacitors, voltage regulators, and mutual impedances.

This model can be applied in three-phase OPF assessments on transmission or distribution networks. In this paper we have applied it to active distribution networks, where unbalanced loads are frequent, distributed generation is presented, and the R/X ratio is generally high; thus, a complex formulation is usually necessary. Therefore, the proposed model may help to simplify the complexity of the OPF formulations for ADN's.

The proposed formulation also may be extended to many other power system problems, such as static and dynamic stability analysis, operation, expansion planning, and others. It provides effective and promising results with high computational performance, it is easy to be implemented, and it is applied in many types of unbalanced loads.

Table 1. Summary of related works and the proposed work with formulation features. N denotes “no”, and Y “yes”

work	P/I	S/T	SC	LF/OPF	MI	LP	CP	VR
[6]	P	T	N	LF	N	Y	N	N
[7]	P	T	N	LF	Y	Y	Y	N
[8]	P	T	N	LF	Y	Y	N	N
[9]	P	S	-	LF	-	Y	N	N
[10]	I	T	N	LF	N	Y	N	N
[11]	I	T	N	LF	Y	N	N	N
[12]	I	T	N	LF	N	N	N	N
[13]	I	S	-	OPF	N	Y	Y	N
[14]	I	T	N	LF	N	Y	Y	Y
[15]	I	T	Y	OPF	N	Y	N	N
[16]	P	S	-	OPF	-	Y	N	N
[17]	P	S	-	LF	-	-	Y	N
[18]	P	S	-	OPF	-	N	Y	N
[19]	P	T	N	OPF	Y	N	Y	Y
Proposed Model	I	T	N	OPF	Y	Y	Y	Y

Contributions

This paper presents the following contributions, which can be observed in Table 1:

i. A simple and efficient model for calculating the L-3φ-ACOPF current injection-based for unbalanced ZIP loads considering capacitors and voltage regulators;
ii. Using [10] as a reference, we propose its extension to the OPF, eye and delta loads, capacitors, and voltage regulators;
iii. Inclusion of mutual impedance in the formulation;
iv. Application of (i) in an active distribution network with high distributed generation penetration and a high R/X ratio;
v. Comparisons of simulation results of our proposed L-3φ-ACOPF model with a nonlinear three-phase ACOPF (NL-3φ-ACOPF) model.

METHODOLOGY

Basic Formulation

In order to illustrate all inbound and outbound currents in the power system,
Figure **1** presents the current flow in a generic node of a phase (adapted from [20]):

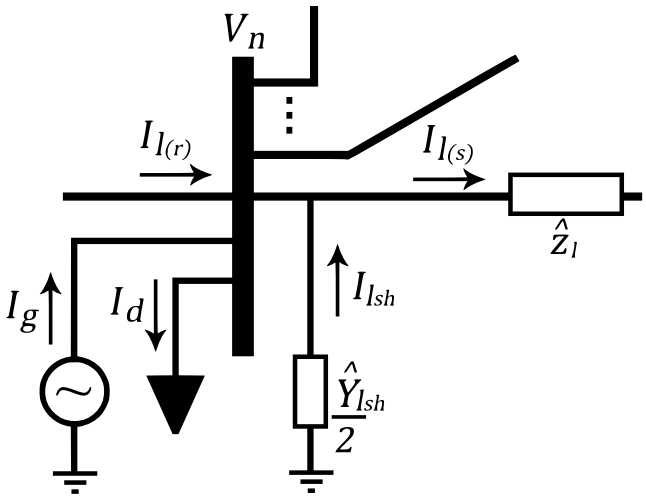

Figure 1. Generic bus of a phase with the current flow (adapted from [20])

From
Figure **1**, the following equations are defined:

$$\sum_{g} I_g - \sum_{l} \left(I_l - I_{l_{sh_s}}\right) + \sum_{l \epsilon \Omega^L_{n(r)}} \left(I_l + I_{l_{sh_r}}\right) - \sum_{d \epsilon \Omega^D_n} I_d = 0 \quad (1)$$

$$V_{n(r)} = V_{n(s)} - \hat{z}_l \, I_l \quad (2)$$

$$I_{l_{sh}} = -V_n \, \hat{Y}_{l_{sh}}/2 \quad (3)$$

$$\left|S_g\right| \leq \left|\hat{S}_g^{max}\right|, \text{ or, } \left|V_n I_g^*\right| \leq \left|\hat{S}_g^{max}\right| \quad (4)$$

Where n is a node in the power system. I_g, I_d, I_l, and $I_{l_{sh}}$ represent the current provided by the generator, the current consumed by the load, the current that flows through the lines, and the current provided by the shunt admittance, respectively. The sets Ω_n^G, $\Omega_{n(s)}^L$, $\Omega_{n(r)}^L$, and Ω_n^D represent the following components connected to node n: generators, sending end of lines, receiving end of lines, and loads, respectively. $V_{n(s)}$ and $V_{n(r)}$ are the voltage in the sending end of lines and receiving end of the line, respectively. $\hat{z}_l$ is the line impedance and $\hat{Y}_{l_{sh}}$ is its shunt admittance. S_g is the apparent power generated in the generator unit g and $\hat{S}_g^{max}$ is the maximum power in generator g.

Equations (1) to (4) use complex numbers and their variables are in rectangular form. Equation (1) denotes Kirchhoff's current law in any node n. The voltage drop in the line is represented in (2). Equation (3) represents the current in the shunt admittance in the line. And the apparent power limit in the generator is presented in (4).

Figure **2** is presented a generic delta and grounded wye loads. The phase impedances are represented by the index dz. And I_{dz} denotes the current that flows through the impedance z_{dz}.

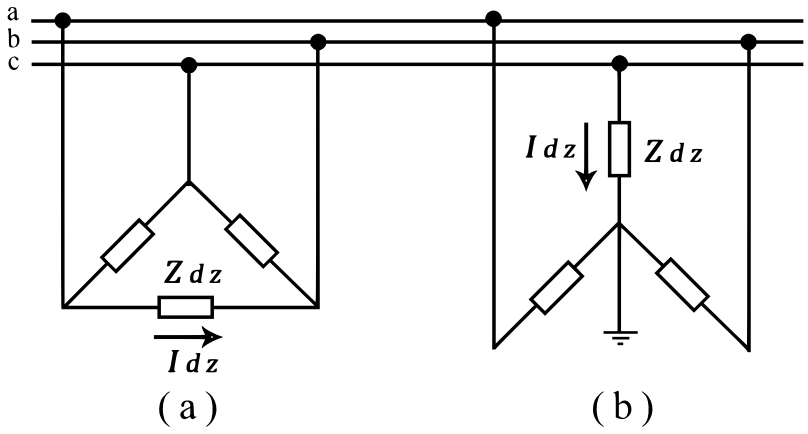

Figure 2. Delta (a) and Grounded Wye (b) load representation

Considering V_{dz} as the voltage over the impedance z_{dz}, the current I_{dz} is calculated by (adapted from [10]):

$$I_{dz} = \hat{\mu}_z \frac{V_{dz}}{\hat{z}_{dz}} + \hat{\mu}_i \hat{I}_{dz} + \hat{\mu}_P \frac{\hat{S}_{dz}}{V_{dz}} \quad (5)$$

where $\hat{\mu}_z$, $\hat{\mu}_i$, and $\hat{\mu}_P$ are known binary variables. $\hat{\mu}_z$ is 1 if the load has constant impedance; 0 otherwise. $\hat{\mu}_i$ is 1 if the load requires constant current; 0 otherwise. $\hat{\mu}_P$ is 1 if the load consumes constant power; 0 otherwise.

Linear Approximations

Equation (4) and the third term in (5) are nonlinear due to the term $1/V$. In [10] is presented the following linearization by neglecting high order terms in its Taylor series. If $V = 1 - \Delta V$, the following linearization is defined:

$$\frac{1}{V} = \frac{1}{1-\Delta V} \approx 1 + \Delta V = 2 - V \tag{6}$$

The error provided by the linearization in (6) is considerably small within voltage limits close to 1 pu. Figure 3 shows the comparison between the expected value (1/V) and the proposed linearization (2-V), as well as the error provided by this approximation.

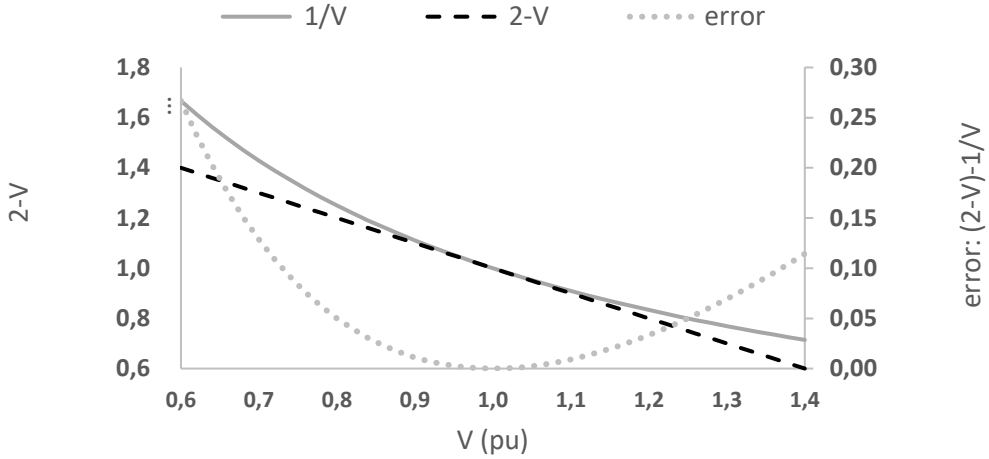

Figure 3. Comparison for the linear approximation 1/V = 2-V

Thus, this work proposes an extension of the linearization presented in [10], which provides small errors for voltage limits near 1 pu. The proposed work includes the formulation of OPF, eye and delta load, capacitors, voltage regulators, and mutual impedance in the model presented in [10].

Linear AC Three-Phase Optimal Power Flow

From the basic formulation and the linear approximation presented in this work, the proposed L-3φ-ACOPF for unbalanced ZIP loads is defined as:

$$min \sum_{\alpha \in \Omega^{\Lambda}} \sum_{g \in \Omega^{G}} \hat{C}_g^G \; Re\left(I_g^{\alpha}\right) \tag{7}$$

subject to:

$$\sum_{g \in \Omega_n^G} I_g^{\alpha} - \sum_{l \in \Omega_{n(s)}^L} \left(I_l^{\alpha} - I_{l_{sh_s}}^{\alpha}\right) + \\ + \sum_{l \in \Omega_{n(r)}^L} \left(I_l^{\alpha} + I_{l_{sh_r}}^{\alpha}\right) - \sum_{d \in \Omega_n^D} I_d^{\alpha} = 0 \qquad \forall n, \forall \alpha \tag{8}$$

$$V_{n(r)}^{\alpha} = V_{n(s)}^{\alpha} - \hat{z}_l^{\alpha} \; I_l^{\alpha} \qquad \forall \alpha, \forall l \tag{9}$$

$$I_{l_{sh_{n(l)}}}^{\alpha} = -V_{n(l)}^{\alpha} \; \hat{Y}_{l_{sh_{n(l)}}}^{\alpha} / 2 \qquad \forall \alpha, \forall l, n(l): \{s, r\} \tag{10}$$

$$I_{dz} = \hat{\mu}_z \frac{V_{dz}}{\hat{z}_{dz}} + \hat{\mu}_i \hat{I}_{dz} + \hat{\mu}_P \hat{S}_{dz} (2 - V_{dz}) \qquad \forall d, \forall dz \in d \tag{11}$$

$$I_d^{\alpha} = I_{dz} \qquad \forall \alpha, \forall d \in \Omega^{D_Y}, \forall dz \in \Omega_{d,\alpha}^{D_Y} \tag{12}$$

$$V_d^{\alpha} = V_{dz} \qquad \forall \alpha, \forall d \in \Omega^{D_Y}, \forall dz \in \Omega_{d,\alpha}^{D_Y} \tag{13}$$

$$I_d^{\alpha} = I_{dz} - I_{dz_c} \qquad \forall \alpha, \forall d \in \Omega^{D_{\Delta}}, \forall dz \in \Omega_{d,\alpha}^{D_{\Delta}} \tag{14}$$

$$V_d^{\alpha} = V_{dz} - V_{dz_c} \qquad \forall \alpha, \forall d \in \Omega^{D_{\Delta}}, \forall dz \in \Omega_{d,\alpha}^{D_{\Delta}} \tag{15}$$

$$Re\left(\hat{V}^{\alpha,min}\right) \leq Re(V_n^{\alpha}) \leq Re\left(\hat{V}^{\alpha,max}\right) \qquad \forall \alpha, \forall n \tag{16}$$

$$Im\left(\hat{V}^{\alpha,min}\right) \leq Im(V_n^{\alpha}) \leq Im\left(\hat{V}^{\alpha,max}\right) \qquad \forall \alpha, \forall n \tag{17}$$

$$-Re\left(\hat{I}_l^{\alpha,max}\right) \leq Re(I_l^{\alpha}) \leq Re\left(\hat{I}_l^{\alpha,max}\right) \qquad \forall\alpha, \forall l \qquad (18)$$

$$-Im\left(\hat{I}_l^{\alpha,max}\right) \leq Im(I_l^{\alpha}) \leq Im\left(\hat{I}_l^{\alpha,max}\right) \qquad \forall\alpha, \forall l \qquad (19)$$

$$Re(I_g^{\alpha}) \leq Re\left(\hat{S}_g^{\alpha,max}\left(2 - V_{n(g)}^{\alpha}\right)\right) \qquad \forall\alpha, \forall g \in \Omega^G \qquad (20)$$

$$Im(I_g^{\alpha}) \leq Im\left(\hat{S}_g^{\alpha,max}\left(2 - V_{n(g)}^{\alpha}\right)\right) \qquad \forall\alpha, \forall g \in \Omega^G \qquad (21)$$

$$V_{n:ref}^{\alpha} = \cos\left(\frac{2\pi}{3}(\alpha - 1)\right) + j\sin\left(\frac{2\pi}{3}(\alpha - 1)\right) \qquad \forall\alpha \qquad (22)$$

Where α:{1,2,3} represents phases a, b, and c; dz denotes the impedances in load d; Sets Ω^{Λ}, Ω^{D}, and Ω^{G} represent all phases, all loads, and all generators in the system, respectively; Sets Ω^{D_Y} and Ω^{D_Δ} are all wye loads and all delta loads, respectively; Sets $\Omega_{d,\alpha}^{D_Y}$ and $\Omega_{d,\alpha}^{D_\Delta}$ are impedances dz from load d connected to phase α for wye and delta loads, respectively. dz_c is the impedance connected to phase α along with dz, for a delta load; operators Re and Im denote the real and the imaginary part of a complex number, respectively; $\hat{V}^{\alpha,max}$ and $\hat{V}^{\alpha,min}$ are the maximum and minimum voltages in the buses of phase α, respectively; $\hat{I}_l^{\alpha,max}$ is the maximum current in the line l in phase α.

All equations from (7) to (22) use complex numbers and the variables are in rectangular forms.

Equation (7) is the objective function of the problem, which seeks to minimize the total generation cost.

Constraint (8) denotes the Kirchhoff's current law in all nodes and all phases. The voltage drop and the shunt current in the lines, for all phases, are defined in (9) and (10), where s denotes “send” and r “receive”, with the current direction in the lines as reference.

The current that flows in each impedance dz of a load d is defined in (11). In this context, load d is formulated as a set of impedances dz.

Constraints (12) to (15) relate the current and voltage of the impedances dz with the current and voltage in the lines and buses of the system, these constraints depend on the load’s type.

Constraints (16) and (17) define the limits for the voltage in the buses. The current in the lines and the power generation limits are defined from (18) to (21). This approach is similar to the power limits defined in the optimal power flow using power injection, in [13] is used the same method and it is proposed how to calculate the limits for $Re(V_n^{\alpha})$ and $Im(V_n^{\alpha})$.

Lastly, constraint (22) sets the voltage and the angle in the reference bus for all phases.

This formulation does not directly provide the power flow through the lines, but the voltage in the buses, its angles, and the current in the lines. Then, the power flow through the lines may be easily calculated by the nonlinear equation using the output values from the proposed formulation:

$$P_{sr} = V_s^2 g_l - V_s V_r g_l cos\theta_{sr} - V_s V_r b_l sin\theta_{sr} \qquad (23)$$

$$Q_{sr} = -V_s^2(b_l + b_{l_{sh}}) + V_s V_r b_l cos\theta_{sr} - V_s V_r g_l sin\theta_{sr} \qquad (24)$$

Where P_{sr} and Q_{sr} are the active power and reactive power in the line; g_l and b_l denote the conductance and susceptance of the line; θ_{sr} is the difference in the angle between buses *s* and *r*.

Extension to Shunt Capacitor and Voltage Regulator

One of the greatest disadvantages in linear OPF models based on power injection is that the capacitors are typically modeled as a constant power load. On the other hand, using current injection, the capacitor may be modeled as a constant impedance load.

Thus, shunt capacitors are included in the proposed formulation as a constant impedance load. And the additional load current I_{dz} is:

$$I_{dz} = V_{dz}\hat{B}_{dz}^{cap} \qquad \forall dz \text{ in the shunt capacitor} \qquad (25)$$

Where $\hat{B}_{dz}^{cap}$ are the phase susceptance of the shunt capacitor.

This approach is more precise than formulations that model the capacitor as a constant power injection.

Furthermore, voltage regulators may be incorporated in constraints (8) and (9) as follows:

$$\sum_{g\in\Omega_n^G} I_g^\alpha - \sum_{l\in\Omega_{n(s)}^L}\left(I_l^\alpha - I_{l_{sh_s}}^\alpha\right) + \sum_{l\in\Omega_{n(r)}^L}\left(I_l^\alpha \hat{\zeta}_l^{-1} + I_{l_{sh_r}}^\alpha\right) - \sum_{d\in\Omega_n^D} I_d^\alpha = 0 \qquad \forall n, \forall\alpha \quad (26)$$

$$V_{n(r)}^\alpha = \hat{\zeta}_l \; V_{n(s)}^\alpha - \hat{z}_l^\alpha \; I_l^\alpha \qquad \forall n, \forall\alpha \quad (27)$$

Where $\hat{\zeta}_l$ is a complex number that represents the voltage regulator in the line l. $\left|\hat{\zeta}_l\right|$ is equal to the tap-changer and the angle $\measuredangle\hat{\zeta}_l$ is the phase shifting.

Extension to Mutual Impedance

The effects of mutual impedance in AC three-phase transmission and distribution lines are widely known and may considerably impact the OPF calculation if not formulated properly.

In [8] is presented the formulation of mutual impedance for the L-3φ-ACOPF based on power injection, where the power flow equations are extended to the mutual impedance, introducing a power flow through lines connecting the phases. The same approach is used in this work, but for the OPF formulation based on the current injection. Thus, the mutual impedance may be incorporated in constraints (8) and (9) as follows:

$$\sum_{g\in\Omega_n^G} I_g^\alpha - \sum_{l\in\Omega_{n(s)}^L}\left(I_l^{\alpha\beta} - I_{l_{sh_s}}^{\alpha\beta}\right) + \sum_{l\in\Omega_{n(r)}^L}\left(I_l^{\alpha\beta} + I_{l_{sh_r}}^{\alpha\beta}\right) - \sum_{d\in\Omega_n^D} I_d^\alpha = 0 \qquad \forall n, \forall\alpha, \forall\beta \quad (28)$$

$$V_{n(r)}^\alpha = V_{n(s)}^\beta - \hat{z}_l^{\alpha\beta} \; I_l^{\alpha\beta} \qquad \forall n, \forall\alpha, \forall\beta \quad (29)$$

Where α and β represent all phases in the system. $I_l^{\alpha\beta}$ is the current in line l if α=β and the current in the mutual impedance if $\alpha\neq\beta$. $\hat{z}_l^{\alpha\beta}$is the impedance in line l if α=β and the mutual impedance if $\alpha\neq\beta$.

CASE STUDY, RESULTS AND DISCUSSIONS

The proposed methodology is illustrated using the IEEE 123-bus test system [21], which includes unbalanced loads, capacitors, and voltage regulators.

The test system is illustrated in different scenarios. Firstly, it is performed a case study including the shunt capacitors and neglecting the voltage regulators. Afterward, a second case including the voltage regulators is presented. Then, a new case including distributed generation is examined. And a case considering a high R/X ratio is performed. Finally, a case including mutual impedance is discussed.

All simulations are compared to the results obtained using a nonlinear 3φ-ACOPF presented in [19]. This comparison aims to present the effectiveness of the proposed model and highlight its accuracy.

The numerical experiments for the proposed model are carried out using Gurobi in Python, in a computer with 4 cores and 8GB of RAM memory.

Results Neglecting Voltage Regulators

In this case study, the proposed methodology is applied in the IEEE 123-bus test system, neglecting voltage regulators. Figure 4 presents the results for voltage magnitude and the active power flow provided by the proposed methodology, as well as the results presented in the nonlinear model in [19]. The processing time was 0.009 seconds for the proposed linear model and 1.15 seconds for the nonlinear model.

Figure 4 shows accurate results. The comparison of the nonlinear model with the linear model is important because some linear approximations may provide significant errors. Furthermore, the expected real values of the variables are closer to the results obtained using the nonlinear model.

The absolute values presented in Figure 4 are not sufficient to quantify the accuracy of the proposed model. Thus, Table 2 presents the MAE (Mean Absolute Error) and the MAPE (Mean Absolute Percentage Error) of voltage magnitude, voltage angle, active power flow, and reactive power flow for the case study.

The errors presented in Table 2 are very small, the highest MAPE is in the reactive power flow and its value is 0.107%. The variables most likely to be analyzed are the voltage magnitude and voltage angle because they are the variables used in the power flow calculation in (23) and (24), these variables have MAPE of 0.009% and 0.062%, which is enormously small.

In addition, the processing time of the linear model was 0.8% of the nonlinear model, more than a hundred times less in terms of processing time. This comparison is an illustration of the advantages of using the proposed model; however, it is expected that linear models perform much faster than nonlinear models.

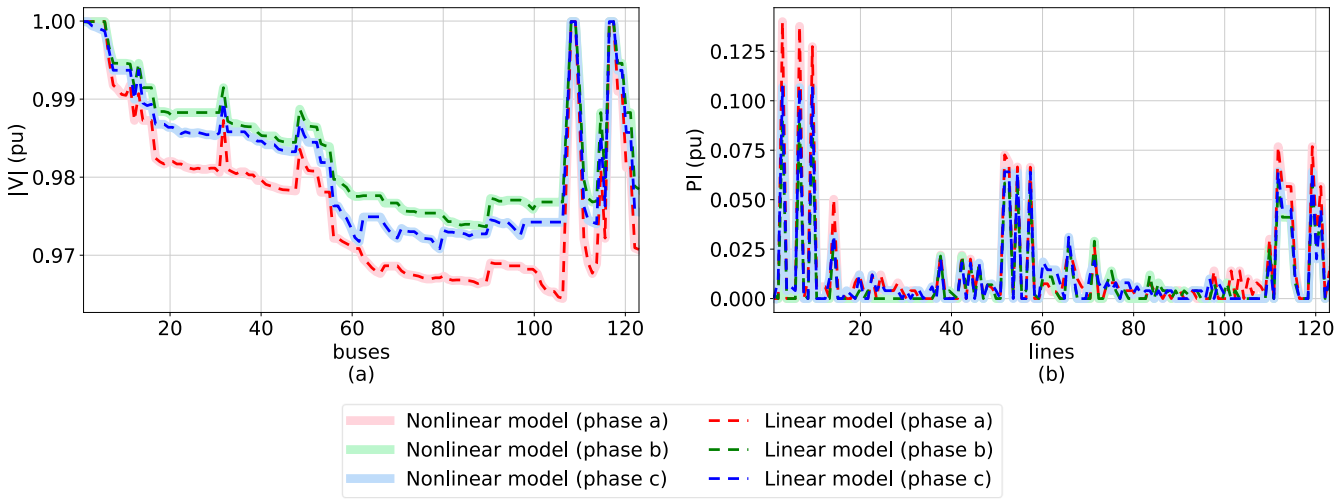

Figure 4. Results from the nonlinear model and the proposed linear model in the 123-bus test system, neglecting voltage regulators

Table 2. MAE and MAPE between linear and nonlinear models for the test system, neglecting voltage regulators.

	MAE	MAPE (%)
Voltage magnitude ($\boldsymbol{V}$)	8.9E-05	0.009
Voltage angle ($\boldsymbol{\theta}$)	1.1E-05	0.062
Active power flow ($\boldsymbol{P_l}$)	1.9E-06	0.007
Reactive power flow ($\boldsymbol{Q_l}$)	1.3E-05	0.107

Results Including Voltage Regulators

In the original IEEE 123-bus test system, there are voltage regulators placed on it.

Figure **5** and Table 3 present the results using the proposed model, including these components. The processing time was 0.011 seconds for the proposed model and 1.16 seconds for the nonlinear model.

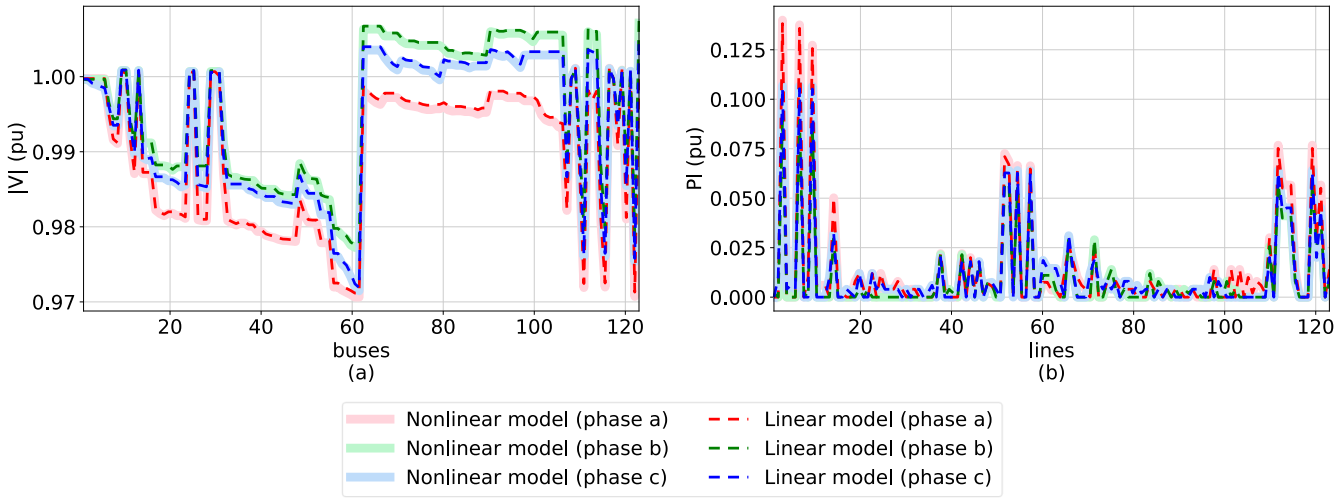

Figure 5. Results from the nonlinear model and the proposed linear model in the 123-bus test system, considering voltage regulators

From

Figure **5**, we observe small errors even if voltage regulators are considered. Compared to Figure 4, we note the voltage increasement in some buses, such as 22, 25, and 62, for both models linear and nonlinear.

The highest MAPE in this case study is 1.36%, and it occurs for the voltage angle. It remains a small error for a linear model.

Table 3. MAE and MAPE between linear and nonlinear models for the test system, considering voltage regulators

	MAE	MAPE (%)
Voltage magnitude ($\boldsymbol{V}$)	6.1E-04	0.061
Voltage angle ($\boldsymbol{\theta}$)	2.2E-04	1.360
Active power flow ($\boldsymbol{P_l}$)	1.2E-04	0.204
Reactive power flow ($\boldsymbol{Q_l}$)	7.6E-05	0.262

Even though the results in Table 3 provide small errors, those errors are higher than the results presented in Table 2. In other words, including voltage regulators in the formulation increases the error comparing the proposed linear model with the nonlinear model; however, the error remains small.

Higher errors after including voltage regulators are expected, since the only linear approximation in this paper, presented in (6), is based on low variations in the voltage magnitude. And the voltage regulators provide additional variation in voltages, which amplifies the error.

Results Including DG

The ADNs are commonly studied in many works due to the integration of distributed energy resources, such as distributed generation (DG). In this case study, it is evaluated the accuracy of the proposed model in a scenario with high penetration of distributed generation. It is considered 12 solar generators placed in the IEEE 123-bus test system, placed on buses 10, 20, 30, 40, …, 110, 120. Each generator has 10 kW of power generation capacity, and each DG unit has a constant power factor equal to 1.

Figure **6.** presents the voltage magnitude and active power flow through the lines for the case study using the linear and the nonlinear model. The processing time was 0.047 seconds for the proposed model and 1.38 seconds for the nonlinear model.

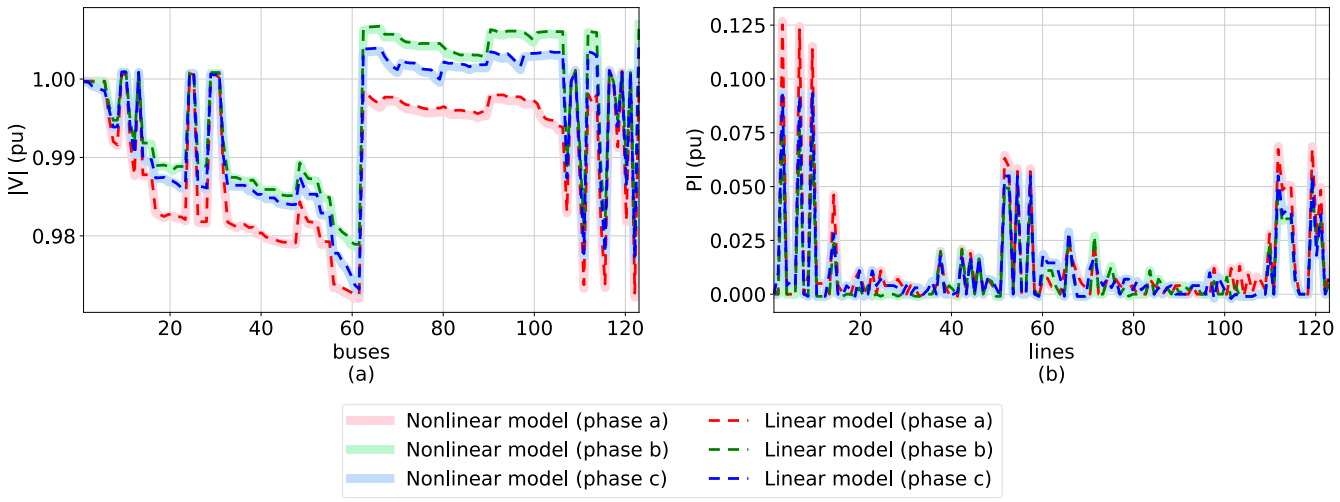

Figure 6. Results from the nonlinear model and the proposed linear model in the 123-bus test system, considering voltage regulators and DG

We note a small deviation in phase c of the voltage magnitude after the voltage regulator (bus 62). This shows that the error in the linearization was amplified after the placement of the distributed generation.

In addition, the absolute values in the power flow through the lines are lower than the cases that do not include DG, because the unit generators can supply the load demand and it is required less power from the grid.

The deviations remain small; however, the analysis of the MAE and MAPE for this case study is necessary and it is presented in Table .

The highest value for the MAPE is 1.29% for the voltage angle. The MAPE value for the voltage magnitude and power flow in the lines is also small, lower than 0.3%.

From these results, it can be concluded that the proposed model can be applied in cases having high penetration of DG, which is the case in ADNs. Also, this model may provide significant computational performance for models developed for the challenges in the ADN.

Table 4. MAE and MAPE between linear and nonlinear models for the test system, considering voltage regulators and distributed generation

	MAE	MAPE (%)
Voltage magnitude ($\boldsymbol{V}$)	5.8E-04	0.058
Voltage angle ($\boldsymbol{\theta}$)	1.8E-04	1.290
Active power flow ($\boldsymbol{P_l}$)	9.9E-05	0.201
Reactive power flow ($\boldsymbol{Q_l}$)	7.2E-05	0.244

Results for High R/X ratio

Distribution power systems may have high values of R/X ratio and this can prevent the use of some linear models, mainly in the ADN.

To understand the behavior and results of the proposed model in cases with a high R/X ratio, for this case study, the resistances of all lines of the IEEE 123-bus test system were multiplied by 10, and its reactances were divided by 10. Therefore, the R/X ratio was increased by 100.

Figure **6** presents the simulation results for the case study. It shows the voltage magnitude and active power flow for the nonlinear and the proposed linear model. The processing time was 0.034 seconds for the proposed model and 1.72 seconds for the nonlinear model.

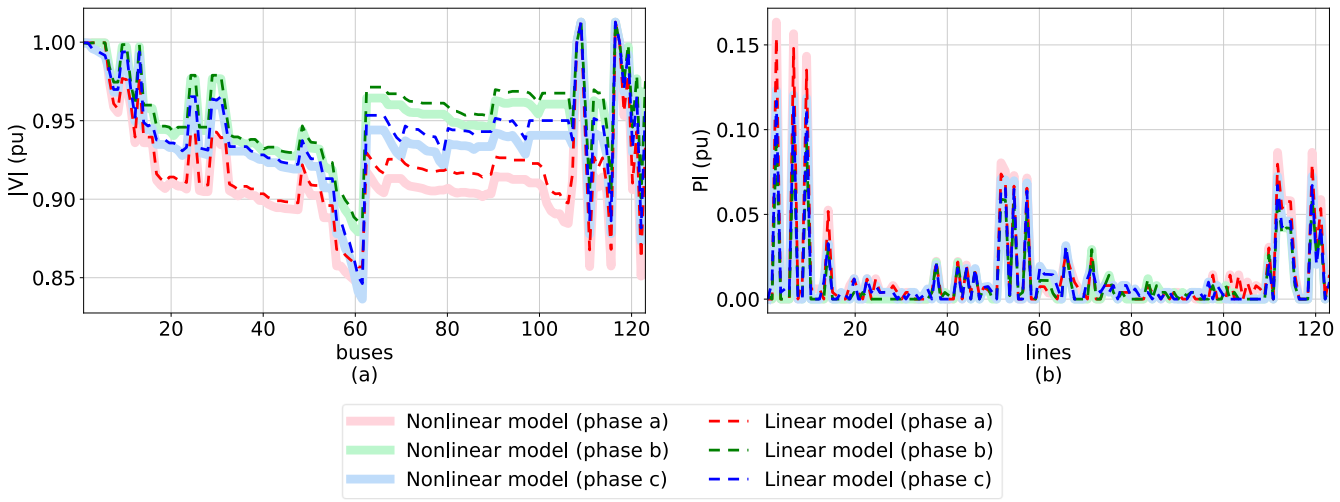

Figure 6. Results from the nonlinear model and the proposed linear model in the 123-bus test system, considering voltage regulators and high R/X ratio

From

Figure **6**, it can be observed an error higher than in the previous case studies. The error may seem to occur after the bus 62, where the voltage regulator is placed. However, the error starts near the bus 55, where the voltage levels are close to 0.85 pu. The error is evident at bus 60, and it remains after bus 62. Thus, we conclude that the only factor that increases the error is high deviations from 1pu in the voltage magnitude.

To correctly evaluate the error in a high R/X ratio, it was created a new case study, only dividing X (reactance of the lines) by 100 and keeping R (resistance of the lines) equal to its original value.

Table 5 and Table 6 present the MAE and MAPE values for high values of the R/X ratio, first for the case having the value of R multiplied by 10, and second for the case keeping the original value of R.

Table 5. MAE and MAPE between linear and nonlinear models for the test system, considering voltage regulators and high R/X ratio (using 10 times R)

	MAE	MAPE (%)
Voltage magnitude ($\boldsymbol{V}$)	6.4E-03	0.639
Voltage angle ($\boldsymbol{\theta}$)	1.7E-03	2.911
Active power flow ($\boldsymbol{P_l}$)	7.0E-04	1.986

Reactive power flow ($\boldsymbol{Q_l}$)	1.7E-04	1.007

Table 6. MAE and MAPE between linear and nonlinear models for the test system, considering voltage regulators and high R/X ratio (keeping R)

	MAE	MAPE (%)
Voltage magnitude ($\boldsymbol{V}$)	3.9E-04	0.039
Voltage angle ($\boldsymbol{\theta}$)	9.7E-04	0.383
Active power flow ($\boldsymbol{P_l}$)	6.6E-04	1.221
Reactive power flow ($\boldsymbol{Q_l}$)	6.9E-05	0.278

We observe that high values for the R/X ratio do not significantly increase the error; however high values of R (resistance) in the lines may provide significant errors in the proposed formulation.

For the case using 10 times R, the error for the voltage magnitude is 0.639%, which is more than 10 times the error in the other study cases, but still acceptable for a linear model.

Results Considering Mutual Impedance

Many linear models for the L-3φ-OPF do not consider mutual impedance, which may considerably increase the expected error.

To illustrate the inclusion of mutual impedance in the proposed formulation, presented in (28) and (29),

Figure **7** shows the comparison of the results for the nonlinear model and the linear proposed model considering mutual impedance. The processing time was 0.055 seconds for the prosed model and 1.29 seconds for the nonlinear model.

From

Figure **7**, we observe an increase in the error, compared with the other case studies presented. That occurs because the inclusion of mutual impedance may increase the voltage difference from one bus to another. Examples are the buses 22-37, in

Figure **7**, the difference in the voltage from one bus to another is up to 200% higher than the values observed in

Figure **5**.

Table 7 presents the MAE and MAPE values for this case study and we note the increase in the error compared to the other case studies.

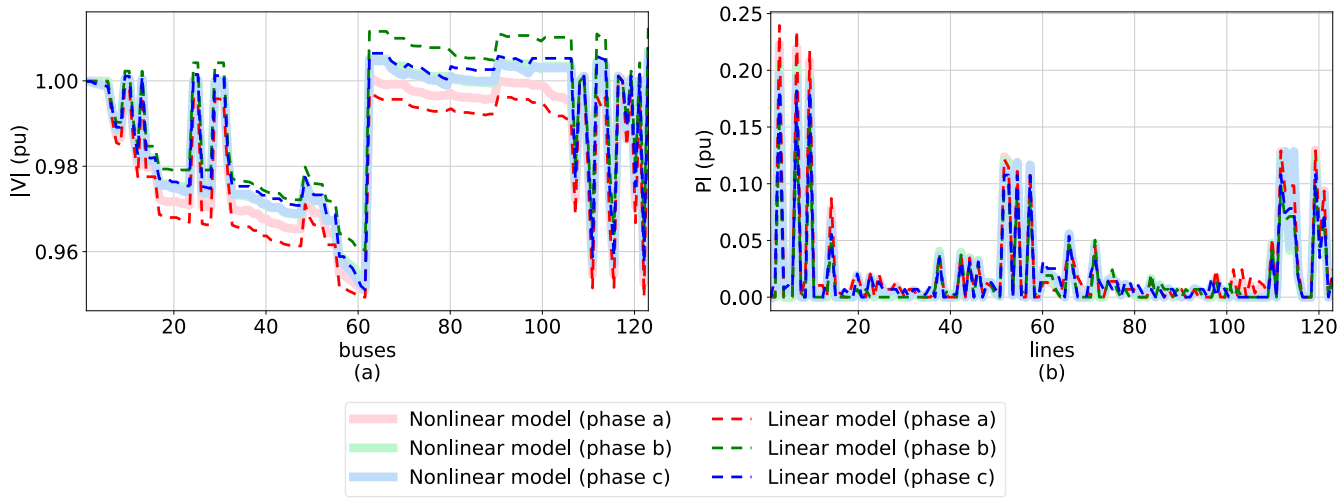

Figure 7. Results from the nonlinear model and the proposed linear model in the 123-bus test system, considering voltage regulators and mutual impedance

Table 7. MAE and MAPE between linear and nonlinear models for the test system, considering voltage regulators and mutual impedance

	MAE	MAPE (%)
Voltage magnitude ($\boldsymbol{V}$)	3.1E-03	0.315
Voltage angle ($\boldsymbol{\theta}$)	2.6E-04	0.941

Active power flow ($\boldsymbol{P_l}$)	3.4E-04	2.667
Reactive power flow ($\boldsymbol{Q_l}$)	1.5E-04	2.645

The errors from this case study, in Table 7, are acceptable for a linear model. The highest error is for the active power flow, which is 2.667%. The errors in the voltage magnitude and voltage angle are lower than 1%.

The errors are higher than in the first and second case studies because it is accumulated the error provided by the inclusion of voltage regulators and the mutual impedance, which increase the variation in the voltage levels, consequently, the error. These results show the accuracy of the proposed linear model, even considering voltage regulators, capacitors, and mutual impedance.

Comparison with other models

The proposed model in this work has provided errors of 8.9E-05 (0.009%) and 1.1E-05 (0.062%) for the voltage magnitude and voltage angle when using the 123-bus test system, respectively. In contrast, the model proposed in [13] shows an error of 4.2E-04 for the voltage magnitude and 5.0E-02 for the voltage angle. In [16], the authors show an error of 1.5% for the voltage magnitude in their proposed linear model.

Traditional linear DCOPF models neglect reactive power flow and voltage magnitude, while the proposed model includes these aspects that are important for active distribution network planning and analysis. The maximum error between the proposed model and the linear DCOPF presented in [22] is 0.081% for the voltage angle and 0.035% for the active power flow using the 123-bus test system.

On the other hand, traditional nonlinear ACOPF models consider the reactive power flow and voltage magnitude but require specific methods to solve nonlinear problems, which are expensive in computational manners. In contrast, our model uses only linear equations and provided a maximum error of 0.062% for the voltage angle and 0.007% compared to the work presented in [19], which proposes an ACOPF model for three-phase power systems. Therefore, the model proposed in this work is simple and fast enough to be incorporated in complex models to study active distribution networks and microgrids, while it provides small errors compared to more complex models.

CONCLUSION

This paper presented a new formulation for the linear AC three-phase optimal power flow for unbalanced ZIP loads. The proposed methodology has the potential to be applied in many power system problems, such as static and dynamic analysis, simulations, and optimization of operation and expansion planning in transmission or distribution systems levels.

The formulation is based on the current injection equations and uses only one linearization in its equations, which shows small errors. The methodology is easy to be implemented and provides high computational performance.

The IEEE-123 bus test system was used to illustrate the methodology in five case studies: firstly, neglecting voltage regulators; secondly, including the voltage regulators; thirdly, including distributed generation; posteriorly, using high R/X ratio; finally, including mutual impedance in the formulation.

The proposed linear model was demonstrated to be valid and accurate, providing low deviations from the expected results. Results were compared with a nonlinear model used as a reference/baseline. The simulations provided a mean percentage error (MAPE) for the voltage magnitude of 0.009% in the first case study, 0.061% in the second case, 0.058% in the third case, 0.639% in the fourth case, and 0.315% in the fifth case study.

The proposed model is also recommended to be applied in active distribution network problems because it has provided small errors in cases with high penetration of distributed generation and cases with a high R/X ratio. For all case studies, the processing time was lower than 0.06 seconds using the IEEE-123 bus test system.

The results show that the presented model provides high accuracy even in a high R/X ratio if the R (resistance of the lines) is not too high. For high values of R, the voltage drop provides a high deviation of the voltage from 1 pu, and linearization errors are increased. Besides, any component that may increase the voltage drop is likely to increase the error as well, since the proposed linearization considers the voltage in the buses close to 1 pu.

This is one of the few works that present a comparison of reactive power in the lines between linear OPF and nonlinear OPF models. That provided a MAPE lower than 0.107% in the first case study, 0.262% in the

second case, 0.244% in the third case, lower than 1.007% in the fourth case, and lower than 2.645% in the fifth case study.

Future works may include energy storage systems, apply the formulation in the expansion planning of active distribution systems and microgrids, and incorporate uncertainties in the formulation.

REFERENCES

1. Stott B, Jardim J, Alsaç O. DC power flow revisited. IEEE Trans Power Syst. 2009;24(3):1290–300.
2. Renato CG. New-method for the analysis of distribution networks. IEEE Trans. Power Deliv. 1990;5(1):391–6.
3. Pinto RS, Unsihuay-Vila C, Fernandes TSP. Multi-objective and multi-period distribution expansion planning considering reliability, distributed generation and self-healing. IET GTD. 2019 Jan 22;13(2):219–28.
4. Attarha A, Amjady N, Conejo AJ. Adaptive robust AC optimal power flow considering load and wind power uncertainties. Int J Electr Power Energy Syst [Internet]. 2018 Mar;96(September 2017):132–42. Available from: https://linkinghub.elsevier.com/retrieve/pii/S0142061517317842
5. Yang T. ICT technologies standards and protocols for active distribution network. Smart Power Distribution Systems: Control, Communication, and Optimization. Elsevier Inc.; 2018. 205–230 p.
6. Ju Y, Chen C, Wu L, Liu H. General three-phase linear power flow for active distribution networks with good adaptability under a polar coordinate system. IEEE Access. 2018;6(c):34043–50.
7. Li H, Yan X, Yan J, Zhang A, Zhang F. A three-phase unbalanced linear power flow solution with pv bus and zip load. IEEE Access. 2019;7:138879–89.
8. Wang Y, Zhang N, Li H, Yang J, Kang C. Linear three-phase power flow for unbalanced active distribution networks with PV nodes. CSEE J Power Energy Syst. 2017;3(3):321–4.
9. Yang Z, Xie K, Yu J, Zhong H, Zhang N, Xia QX. A General Formulation of Linear Power Flow Models: Basic Theory and Error Analysis. IEEE Trans Power Syst. 2019;34(2):1315–24.
10. Garces A. A Linear Three-Phase Load Flow for Power Distribution Systems. IEEE Trans Power Syst. 2016;31(1):827–8.
11. Sunderland K, Coppo M, Conlon M, Turri R. A correction current injection method for power flow analysis of unbalanced multiple-grounded 4-wire distribution networks. Electr. Power Syst. Res. 2016;132:30–8.
12. Garcia PAN, Pereira JLR, Carneiro S, Da Costa VM. Three-phase power flow calculations using the current injection method. IEEE Trans Power Syst. 2000;15(2):508–14.
13. Ferreira RS, Borges CLT, Pereira MVF. A flexible mixed-integer linear programming approach to the AC optimal power flow in distribution systems. IEEE Trans Power Syst. 2014;29(5):2447–59.
14. Ahmadi H, Marti JR, Von Meier A. A Linear Power Flow Formulation for Three-Phase Distribution Systems. IEEE Trans Power Syst. 2016;31(6):5012–21.
15. Tan Y, Wang Z. Incorporating unbalanced operation constraints of three-phase distributed generation. IEEE Trans Power Syst. 2019;34(3):2449–52.
16. Yu Y, Hou Q, Ge Y, Liu G, Zhang N. A Linear LMP Model for Active and Reactive Power with Power Loss. iSPEC 2019 - 2019 IEEE Sustainable Power and Energy Conference: Grid Modernization for Energy Revolution, Proceedings. 2019;1699–704.
17. Wang Y, Wu H, Xu H, Li Q, Liu S. A general fast power flow algorithm for transmission and distribution networks. IEEE Access. 2020;8:23284–93.
18. Hariharan T, Mohana Sundaram K. Multiobjective optimal power flow using Particle Swarm Optimization. Int. J. Control. Theory Appl. 2016;9(2):671–9.
19. Baran AR, Fernandes TSP. A three-phase optimal power flow applied to the planning of unbalanced distribution networks. Int. J. Electr. Power Energy Syst. [Internet]. 2016;74:301–9. Available from: http://dx.doi.org/10.1016/j.ijepes.2015.07.004
20. Monticelli A. State Estimation in Electric Power Systems. Boston, MA: Springer US; 1999. 368 p.
21. Kersting WH. Radial distribution test feeders. IEEE Trans Power Syst. 1991;6(3):975–85.
22. Helseth A. A Linear Optimal Power Flow Model Considering Nodal Distribution of Losses. 9th International Conference on the European Energy Market. 2012;1–8.